Al-Azhar University Civil Engineering Research Magazine (CERM)
Vol. (39) No. (3) july, 2017

Experimental and Analytical Investigations of Steel CHS Poles Partially Filled with Concrete

Moamen Khalifa[1], Sherif Ibrahim[1], Amr Shaat[2]

[1]*Department of Structural Engineering, Ain-Shams University, Cairo, Egypt*

[2]*Civil Engineering Program, German University in Cairo, New Cairo, Egypt (On leave from Ain-Shams University)*

ملخص البحث:

تعتبر القطاعات الحديديه الدائريه المفرغه من اكثر القطاعات المستخدمه كعناصر اساسيه فى ابراج الكهرباء ، ابراج الاتصالات بالاضافه الى اعمدة الاناره. ولكن غالبا ما يكون الانهيار بعد حدوث تشكلات جانبيه فى القطاع مما يؤدى الى عدم وصول القطاع الى اقصى مقاومة يستطيع تحملها. زيادة سمك القطاع احد الحلول لتقليل التشكلات الجانبيه مما يؤدى الى زيادة مقاومة القطاع و جسائته ولكن فى نفس الوقت زيادة التكلفه بشكل كبير، ولذلك كان من الافضل البحث عن حل اخر اكثر اقتصاديه وهو ملأ هذه القطاعات بالخرسانه لمنع التشكلات الجانبية وزيادة مقاومة القطاع. عند استخدام هذه القطاعات ككابولى، نجد انه عند ملأ الجزء الموجود ناحية القاعدة (حيث توجد اقصى قيمه لعزم الانحناء) بكمية صغيره من الخرسانه فان ذلك سيكون كافى لزيادة مقاومة القطاع و منع التشكلات الجانبية. الهدف الاساسى من هذا البحث هو الحصول على الطول الامثل للخرسانه المستخدمة للوصول لاقصى مقاومه للقطاع عن طريق الاختبارات المعمليه و ايضا عمل نماذج تحليليه لاستنتاج سلوك القطاعات الحديديه المملؤه جزئيا بالخرسانه.

Abstract

In this study, an experimental investigation of the behaviour of steel tubular poles partially filled with concrete was conducted. A total of nine specimens were tested under flexural loading. The main parameters varied in the tests are: (1) the diameter to thickness ratio (D/t) from 57 to 101, and (2) percent of the filled concrete length measured from the base to the total length of the specimen from 15% to 100%. In some specimens, the partial concrete filling prevented the occurrence of local buckling of steel cross section. An analytical model based on moment curvature analysis was conduct to estimate the ultimate capacity and load-deflection curves of the partially filled steel tubular poles. The predicted capacities and behaviour are in good agreement with experimental results. The analytical model was applied in a parametric study to determine optimum partial filling percent for various (D/t) ratios and steel grades.

- ***KEYWORDS*:** Concrete filled; Steel tube; Circular hollow section; Flexure; Local buckling.

Introduction

Steel poles are used mainly in supporting transmission lines, advertising boards, and for lighting applications. Generally, thin steel sections have a problem of local buckling which is called "Ovalization" of steel tubes. Local buckling causes steel member to fail before reaching the full capacity of the section. Increasing wall thickness of steel pole is an uneconomical solution. Using lower cost material like concrete to prevent the occurrence of local buckling of the steel pole by adding it in the zone of max moment only to avoid a big increase in dead weight. Number of studies [Elchalakani, et al. (2001), Fouad, et al. (2006)] have presented the advantages of fully filled steel poles with concrete, but this solution increases the dead weight significantly. Also there is a number of studies [Fouad, et al. (2006), Mitchell and Fam (2010)] have presented the advantages of partially concrete-filled steel tubes. The main objective of this study is to provide an experimental illustration of this concept for different D/t ratios, and more

importantly, to define analytically the optimal length of concrete filling for each D/t ratio.

1. Experimental Program

The experimental program included testing nine specimens of full and partially concrete-filled steel tubes in cantilever loading pattern, as shown in Fig. 1. The main variables are the percentage of concrete filled portion of the steel tube and the diameter-to-thickness ratio of steel tubes. Table 1 lists the dimensions of all tested poles, D/t ratio, filled length and its percentage with respect to the clear cantilevered length. The following sections provide details of the experimental program and the results.

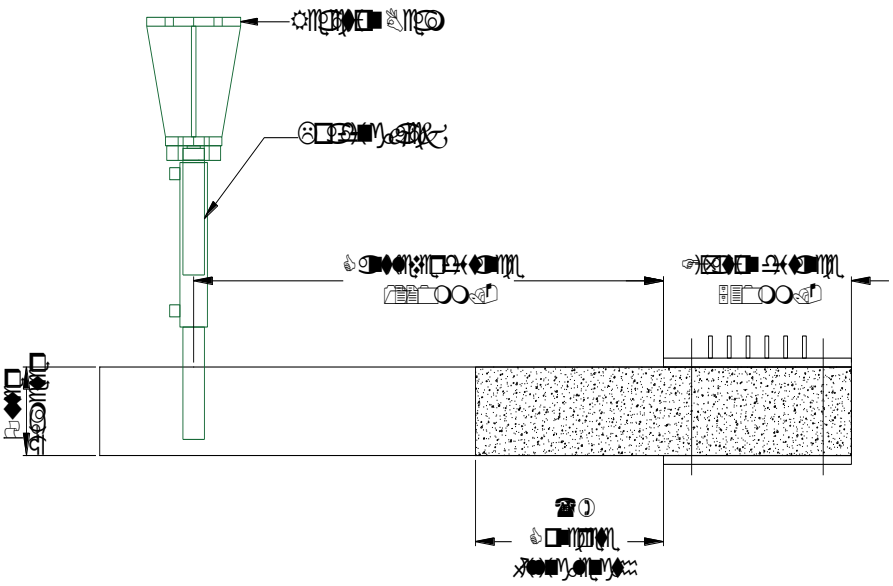

Figure 1: Schematic diagram of test specimens

Table 1: Details of steel tube test specimens

Specimen no.	Outer diameter (mm)	Thickness (mm)	D/t ratio	Concrete length above base (mm)	Concrete filling percentage above base
T114-100	114.3	2	57	1220	100.00 %
T114-36	114.3	2	57	440	36.06 %
T114-16	114.3	2	57	190	15.57 %
T160-100	160	2	80	1220	100.00 %
T160-34	160	2	80	412	33.77 %
T160-16	160	2	80	200	16.39 %
T202-100	202	2	101	1220	100.00 %
T202-39	202	2	101	480	39.34 %
T202-11	202	2	101	140	11.48 %

1.1 Description of Test Specimens and Fabrication

The nine specimens were 2000 mm long, with 114.3, 160, and 202 mm outer diameters (D), and a 2 mm wall thickness (t) with diameter-to-thickness (D/t) ratios of 57, 80, and 101 for groups 1, 2, and 3 respectively.

Based on these D/t ratios, all specimens are classified under the non-compact sections category according to the ANSI/AISC 360-16. The 2000 mm total length is distributed over three parts. The first part is 530 mm long which is considered as the fixed end, the second part is the actual cantilever length which is equal to 1220 mm, while the third part is the remaining length of specimen which is used to apply the load as shown in Fig. 1. All specimens were filled with concrete on the same day from two batches having the same mix. The tubes were propped vertically and secured to scaffolding to allow filling from above. The final height of the concrete fill was measured after the concrete had hardened.

1.2 Materials

Steel Tubes

Mechanical properties of the steel were obtained by cutting longitudinal coupon from each steel tube and testing it under axial tension. Results of mechanical properties are shown in Table 2.

Table 2: Mechanical properties of steel tube based on coupon tests

Property	For D=114.3 mm	For D=160 & 200 mm
Elastic modulus, *E* (GPa)	210	210
Yield strength, f_y (MPa)	440	280
Yield strain	0.0022	0.0017
Ultimate strength, *fu* (MPa)	485	385
Ultimate strain	0.213	0.26

Concrete

All specimens used the same concrete mix. Five 150 x 150 x 150 mm concrete cubes were tested at the same time of testing steel poles. It should be noted that poles testing took place six months after concrete casting, which means that the concrete has almost reached its full strength. The compressive strengths for cubes ranged from 44.5 to 46.67 MPa with an average value of 45.97 MPa. It is worth noting that in flexure, the strength of the concrete fill was shown to have insignificant effect on the flexural strength of concrete-filled tubes and that its primary function is prevention of local buckling [Fam and Rizkalla (2002)].

1.3 Test Setup and Instrumentation

Each specimen was loaded by a single point load at the free end in cantilever bending as shown in Fig.2-a. The fixed support was provided by gripping the 530 mm long concrete-filled end portion of the tube. The tube was placed between two steel plates. The plates were clamped to a rigid steel post using threaded rods as shown in Fig.2-a. Load was applied at a distance of 1220 mm from the face of the fixed base using a manually operated hydraulic jack as shown in Figure 2-b. The load cell was directly positioned below the hydraulic jack and fitted with a spherical cap as shown in Figure 2-b. For partially filled specimens, to avoid ovalization and local crushing of the steel tube at the loading point, a vertical steel stiffener plate was inserted inside the tube as well as an external plate is welded to the specimen from the outside (Figure 2-c). A steel rod was used between the loading end of the jack and the tube to facilitate free rotation as shown in Fig. 2-b. Deflection was measured at the loaded end using two LVDTs from both sides (LVDT 1 and 2), and one LVDT at the end of hollow part (LVDT 3) was used in partially filled specimens as shown in Fig. 3-a. Also, two LVDTs are used to record any rotation occurred to the fixed post (LVDT 4 and 5), as shown in Fig. 3-b.

Longitudinal strains were measured at various locations, including the extreme compression and tension fibers at the fixed end (SG1 and SG2) and the tension side at the end of hollow part (SG3) using electric resistance strain gauges as shown in Fig. 3-c.

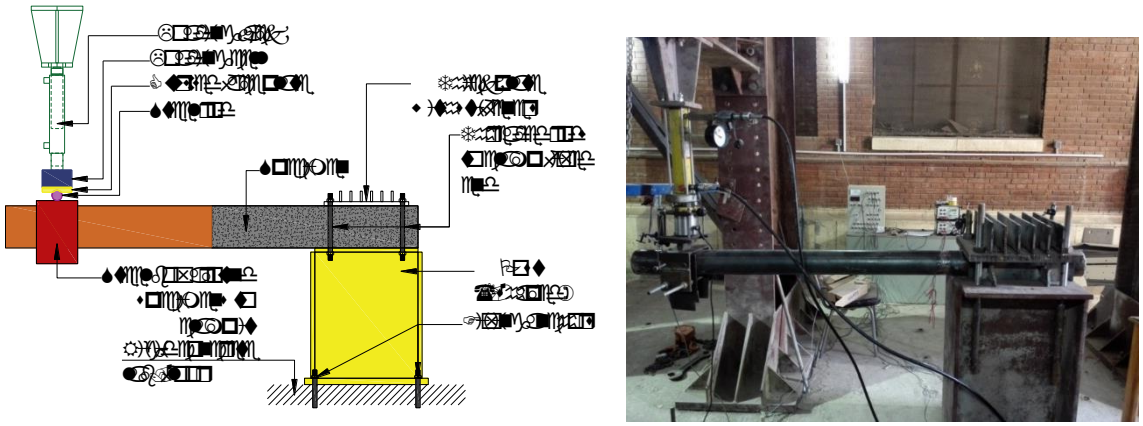

(a) Test setup

(b) Loading jack details

(c) Details at point of loading to avoid crashing of tube and local buckling

Figure 2: Test setup

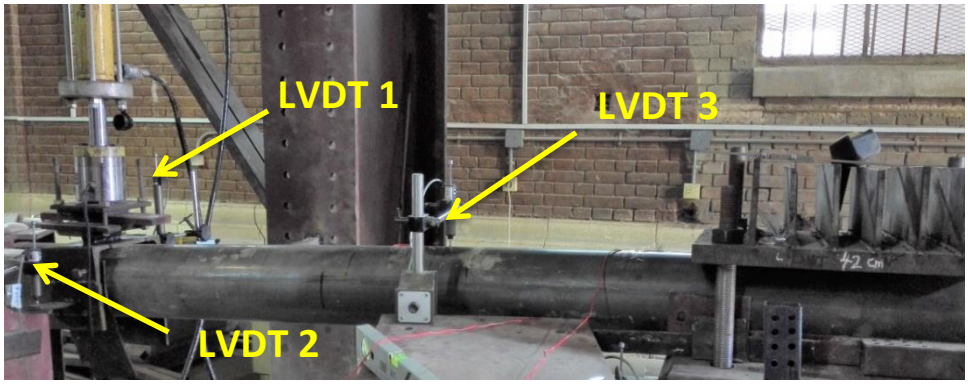

(a) Position of LVDTs

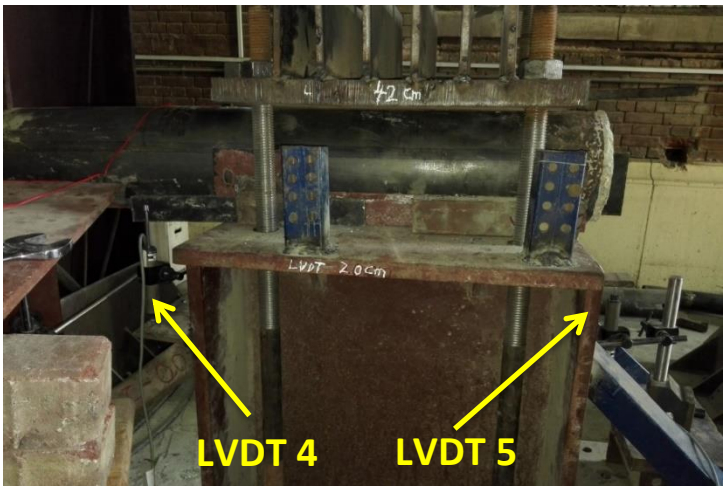

(b) LVDTs used to record rotation of the fixed post

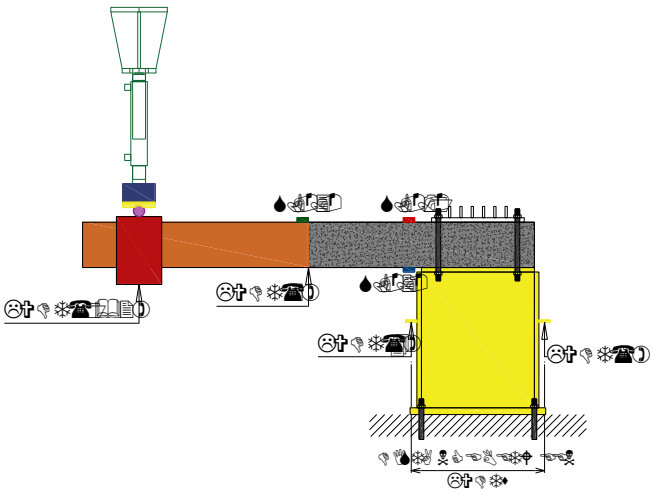
(c) Schematic of test instruments

Figure 3: Test instruments

1.4 Experimental Results

1.4.1 Load-deflection behaviour

Fig. 4 shows the load-deflection responses for each (D/t) ratio group which consists of three specimens. The benefit of increasing concrete filled length, in terms of increasing the ultimate load and flexural stiffness is clearly demonstrated. It is worth noting that

the ultimate deflection of Specimens T114-100 and T114-36, which have the same failure mode, is almost similar. This is because the hollow part was rather close to the zero moment regions, where curvatures are insignificant. Table 3 summarizes experimental results. Stiffness began to decrease when the steel tube started to yield. For test specimens with (D/t) ratio of 57, a filling ratio of 36% prevented the occurrence of local buckling failure. However, for groups with (D/t) ratios 80 and 101, a partial filling up to 39% have not prevented local buckling.

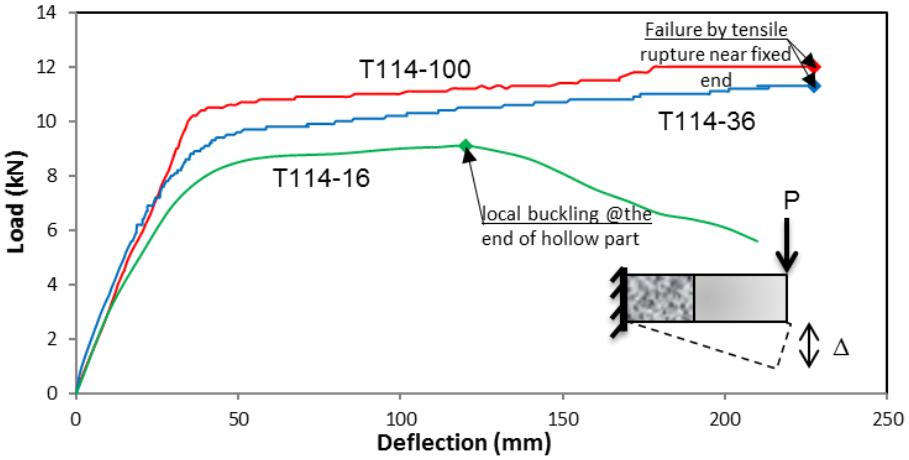

(a)

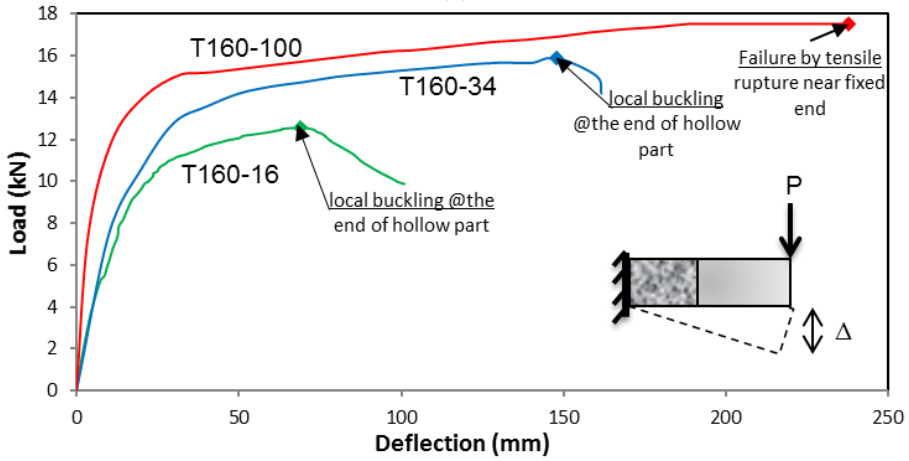

(b)

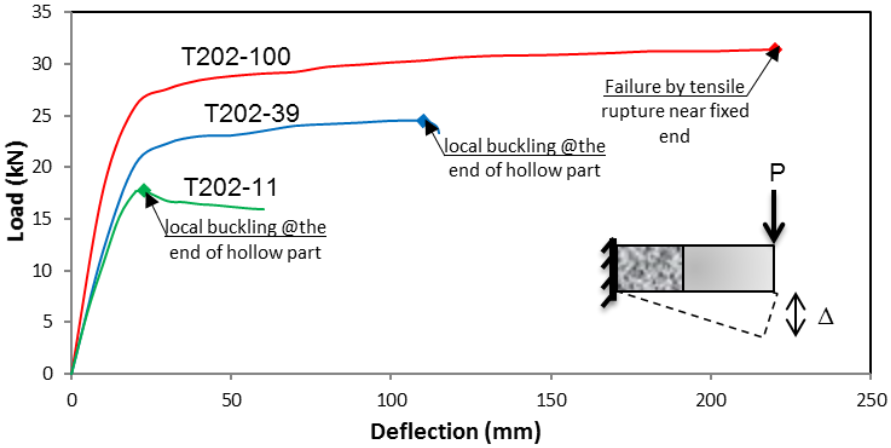

(c)

Figure 4: Load-deflection behavior of the three tested groups

Table 3: Summary of experimental results

Specimen no.	Max. load (kN)	Corresponding deflection (mm)	Initial stiffens (N/mm)	Initial stiffens / filled specimen initial stiffens
T114-100	12	227.0	288	100.00 %
T114-36	11.3	227.6	286	99.30 %
T114-16	9.1	125.2	225	78.13 %
T160-100	17.5	237.5	950	100.00 %
T160-34	15.9	149.5	700	73.68 %
T160-16	12.6	69.0	620	65.26 %
T202-100	31.5	219.4	1950	100.00 %
T202-39	24.6	103.9	1200	61.54 %
T202-11	17.8	22.7	1050	53.85 %

1.4.2 Failure modes

The amount of concrete filling affected the failure mode and its location. The specimens with short filled length failed at the hollow part, while the fully filled specimens failed at the fixation. Failure of the concrete-filled sections occurred generally on the tension side near the base by rupture of the specimen as specimens T114-100, T114-36, T160-100, and T202-100 (Figure 5-a). Failure of the hollow sections occurred by local buckling of steel tubes at compression side almost at the concrete face as specimens T114-16, T160-34, and T202-39 (Figure 5-b). Specimens T160-16, and T202-11 which have a very short filled length failed by local buckling of steel tubes at compression side near the concrete face inside the filled part with a distance almost equal half the diameter (Figure 5-c).

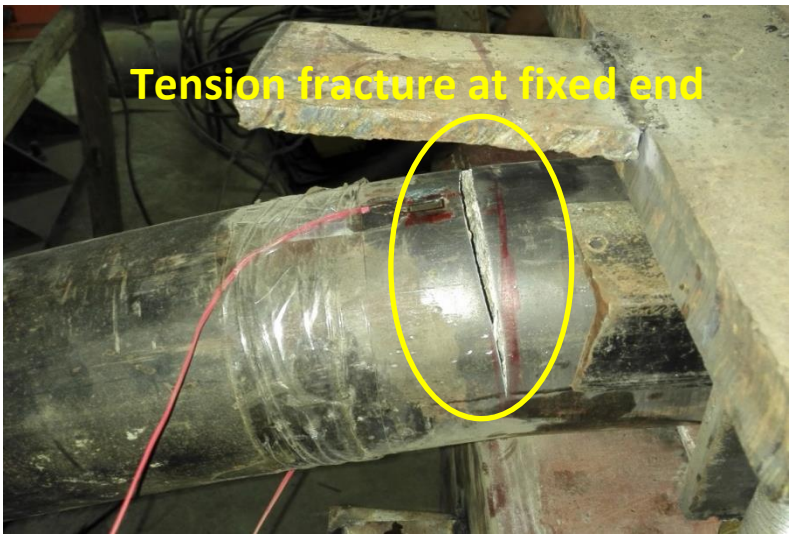

(a)

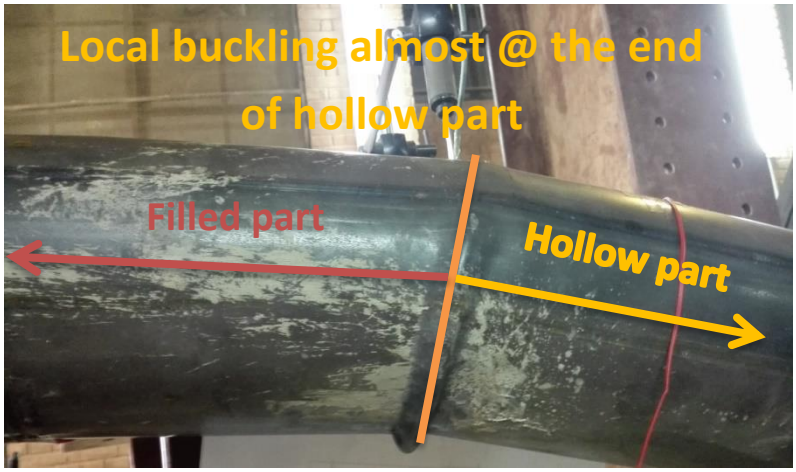

(b)

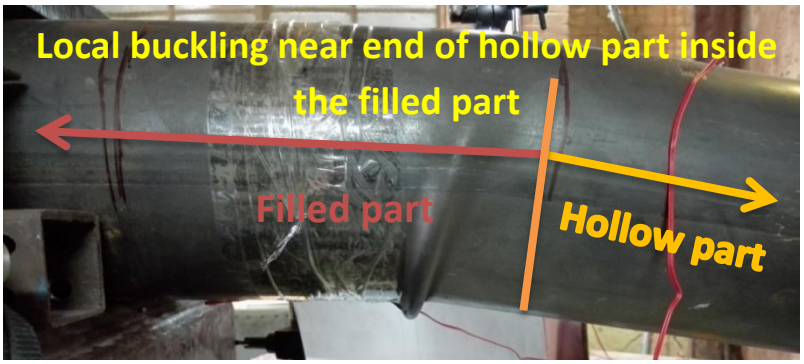

(c)

Figure 5: Modes of Failure

1.4.3 Load-strain behaviour

Fig. 6 shows the load-strain responses of each (D/t) ratio group. Axial strains were measured at the base of each tube on both the compression and tension sides, also, at the end of hollow part at tension side. Not all the curves were completed due to instrumentation malfunction slightly below the maximum load. The load-strain relationship is similar to that of the load-deflection. Greater strains were achieved for specimens having higher concrete filling ratio. Each specimen yielded in tension before yielding in compression. It's noticed that the filled length affects the distribution of the strain along the length of the specimen. Before yielding, the strain at the fixed base and at the end of hollow part increases in proportion until the strain reaches yield strain in one of the two sections then the distribution of the strain changes. For specimens with long concrete filled lengths as (T114-36), the section at the fixed base reached yielding first which led the strain at the base to increase excessively and the strain at the end of hollow part decreased or stabilized until the section at the fixed end reached the ultimate strain and failed with tensile fracture. On the other hand, for specimens with short concrete filled lengths as (T114-16, T160-16, T202-11), the section at the end of the hollow part reached yielding first which led the strain at the end of the hollow part to increase excessively and the strain at the fixed end decreased or stabilized, then the specimen buckled near the end of the hollow part and the load decreased gradually. For specimens (T160-34, T202-39) with moderate concrete filled lengths, the section at the fixed base reached yielding first and the strain at the base increased excessively beyond

the yield strain, while the strain at the end of hollow part decreased. Upon further loading the strain at the end of hollow part began to increase again and reached yielding after few load steps then local buckling occurred in the compression side of the end of the hollow part.

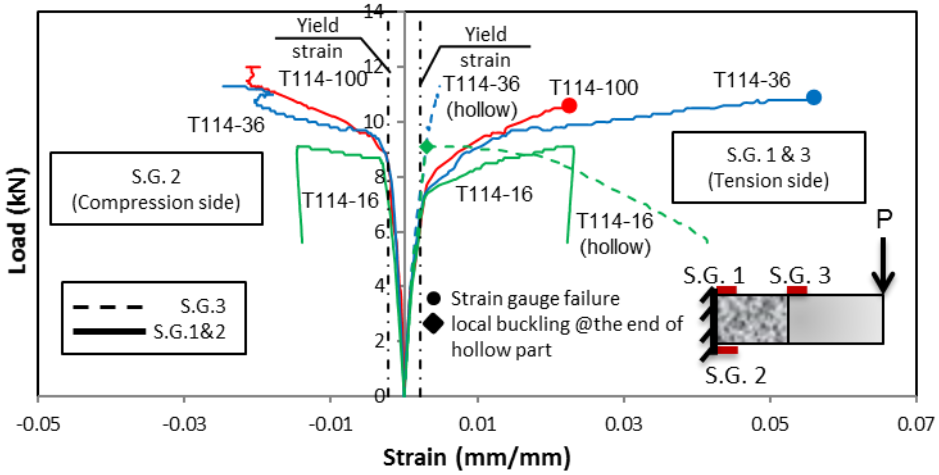

(a)

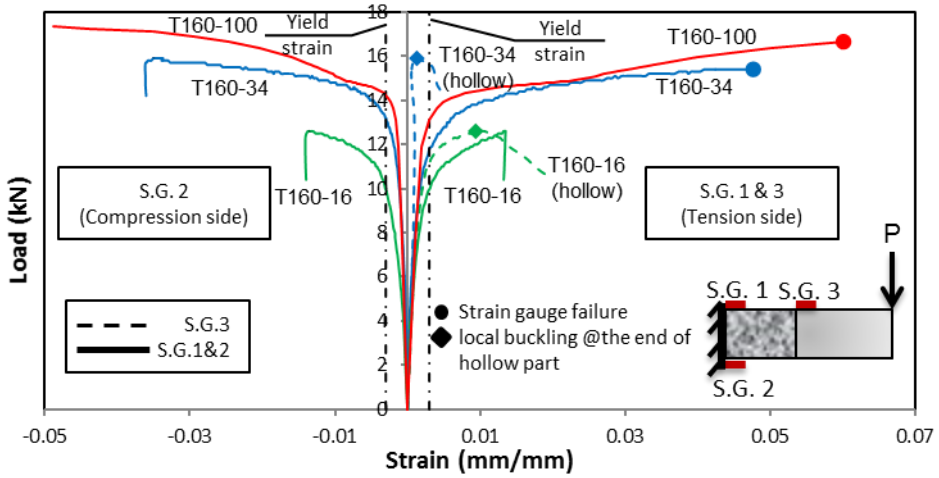

(b)

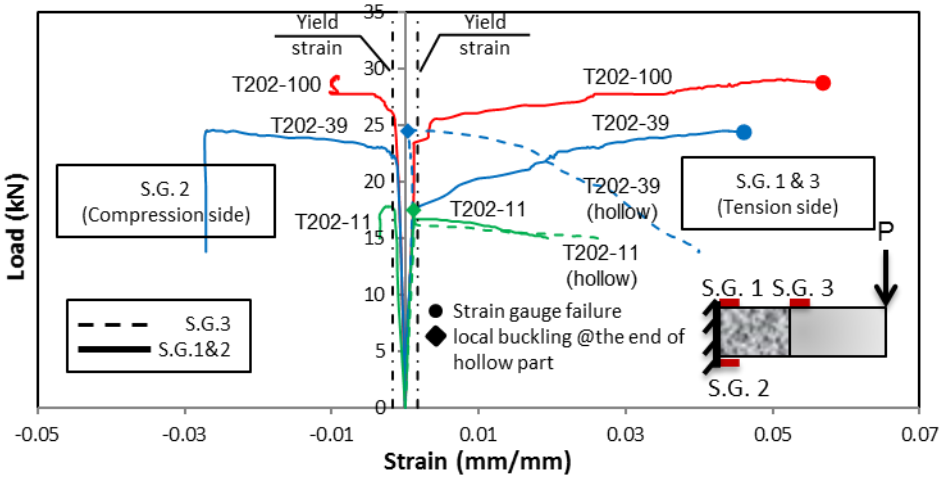

(c)

Figure 6: Load-strain behavior of the three tested groups

Analytical Model

2.1 Moment-Curvature Response of Concrete-Filled Tube

The analytical model is based on the assumption that plane sections remain plane when subjected to bending. This assumption allows the strain to be distributed linearly through the cross-section. Strain compatibility (i.e. full bond) between the tube and the inner core was also assumed. Previous studies by Fam and Rizkalla (2002), Cole and Fam (2006), and Qasrawi and Fam (2008) have adopted and validated these assumptions for FRP tubes. The member is assumed to be cracked under a general bending moment, *M*. The moment-curvature response is complete when the tube material ruptures. The nonlinear stress-strain behaviour of the concrete in compression was modelled by Popovics (1973) and is used in this study, assuming extended strain softening (i.e. curve is not terminated at 0.003 strain) as suggested by Fam and Rizkalla (2002) to account for partial confinement in flexure.

2.2 Moment-Curvature Response of Hollow Tube

This section presents the model that was developed by Brazier (1927) for hollow steel tubes. Modelling hollow tubes is slightly more complex than concrete-filled tubes because cross-sectional ovalization must be accounted for. Brazier introduced second-order effects to the analysis of tubes in flexure to derive the following relationship between the ovalization ratio and normalized curvature:

$$\xi_o = \left(\frac{\psi}{\Psi_N}\right)^2 \quad (1)$$

Where ξ_o is the maximum ovalization ratio, ψ is the applied curvature, and the normalizing factor, Ψ_N, is equal to:

$$\Psi_N = \frac{t}{r^2\sqrt{1-\mu^2}} \quad (2)$$

Where μ is Poisson's ratio for steel, r and t are the radius and thickness of the tube, respectively.

The model for the hollow steel tube is structured similarly to the concrete-filled tube model, in that it adopts a layer-by-layer approach. But since the absence of concrete allows the cross-section to ovalize, the model had to account for the changing geometry. Guarracino (2003) showed that the ovalized cross-section very closely resembles an ellipse, so an elliptical geometry was applied to the deformed section. Ovalization is assumed to have a sinusoidal distribution along the length of the hollow tube (L_h), as adopted by Ibrahim and Polyzois (1999) for cantilevered FRP tubes (Figure 7):

$$\xi(x_h) = \xi_o \sin\left(\frac{\pi x_h}{L_h}\right) \quad (3)$$

where ξ_o is the maximum ovalization at the middle of hollow length, and $\xi(x_h)$ is the ovalization anywhere (distance x_h from the free end) along the hollow length of the tube. The average depth of the initial, un-deformed circular section, D_{av}, is given as:

$$D_{av}=D-t \quad (4)$$

where D is the outer diameter of the section, and t is the structural wall thickness of the tube. Once ovalization begins, the depth, D_v, and width, D_h, become:

$$D_v=D_{av}(1-\xi(x_h)) \quad (5)$$

$$D_h=D_{av}(1+\xi(x_h)) \quad (6)$$

where D_v, and D_h are the center line diameters in the vertical and horizontal directions, respectively, of the deformed cross section.

This assumes that the vertical and horizontal ovalization ratios, $\xi(x_h)$, are equal. The hollow length is divided into n_h segments in the longitudinal direction of equal length x_{ih}. Each section is studied taking into consideration that ovalization happens at its position until establishing the complete moment-curvature response for each section, n. The moment curvature completes when the strain at any section (n), $\varepsilon(x_h)$, reaches the critical strain, ε_{crit}. Korol (1979) developed an expression for the critical buckling strain, ε_{crit}, of a hollow steel tube as follows:

$$\varepsilon_{crit} = \frac{4t}{3D}\sqrt{\frac{E_t}{E_s}} \quad (7)$$

Where ε_{crit} is the critical buckling strain, t is the wall thickness, E_t is the tangent modulus of the material, and E_s is the secant modulus. The values E_t and E_s are calculated from the stress-strain curve for steel.

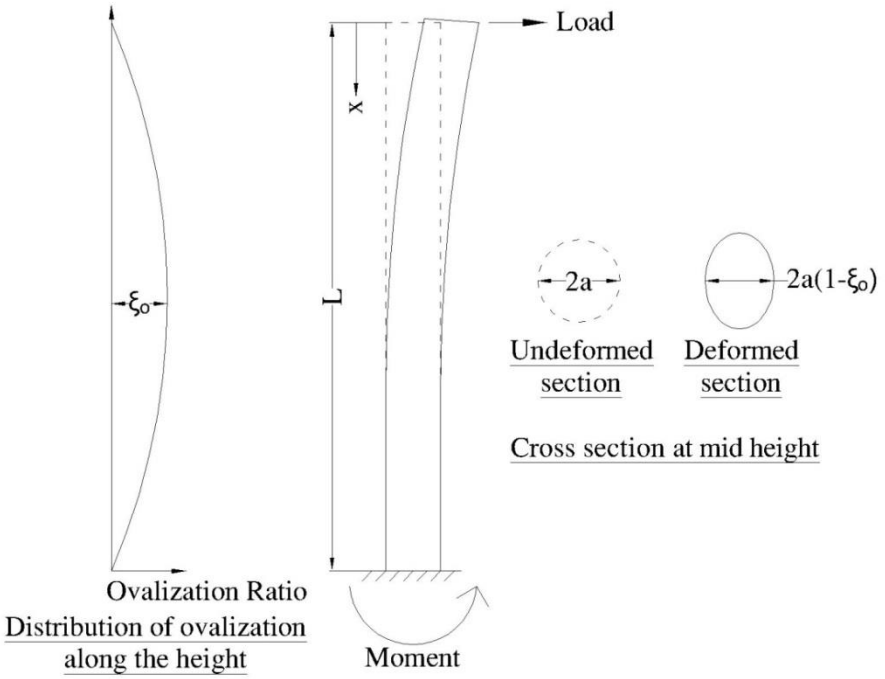

Figure 7: Ovalization of cantilevered tube (adopted from Ibrahim and Polyzois, 1999)

2.3 Load-Deflection Response of Partially Filled Tube

The deflection of the partially filled cantilevered tube is determined by using the moment-area theorem, in which the curvature along the length of the tube is integrated. For a partially filled tube, a bending moment is applied to the fixed end of the cantilever and is linearly distributed along the length. Based on the applied moment anywhere along the length, the corresponding curvature can be calculated from the moment-curvature responses developed for concrete-filled and hollow steel sections. The procedure is summarized as follows:

1. Divide the hollow length, L_h, into n_h sections, where each section, i_h, has equal length x_{ih}. The distance from the tip to any section is $x_h = x_{ih} * i_h$.
2. Apply a moment, M, to the base of the pole. Since the bending moment diagram is linear, the moment in the hollow portion, from the tip to the face of the concrete, is $M(x) = M*(x_h/L)$, where L is the total length of the partially concrete filled tube.
3. For the moment $M(x)$ at each section of the hollow tube, determine the corresponding curvature, $\psi_h(x)$, from the specific moment-curvature response of that section, determined for hollow tube.

4. Check whether the critical strain in Eq. (7) is exceeded at any section along the hollow length.
5. Divide the concrete-filled length into n_f sections, where each section, i_f, has equal length x_{if}. The distance from the tip to any concrete-filled section is $x_f = L_h + x_{if} * i_f$. The bending moment at any section along the concrete-filled portion is $M(x) = M^*(x_f / L)$.
6. Determine the curvature, $\psi_f(x)$, at each section of the concrete-filled portion for the moment $M(x)$ using the moment-curvature response developed for filled section.
7. Check whether the moment at the base, $M(x = L)$, is greater than the ultimate moment for the filled portion that was determined for filled tube. If the ultimate moment is exceeded, the member is failed.
8. Once the curvatures are known along the full length of the pole for the moment M specified in Step 2, calculate the deflection, $y(x)$, using the moment-area method (Figure 8).
9. Return to Step 2 and apply a new moment. Continue until one failure criterion in Steps 4 or 7 is achieved either in the hollow or concrete-filled part.

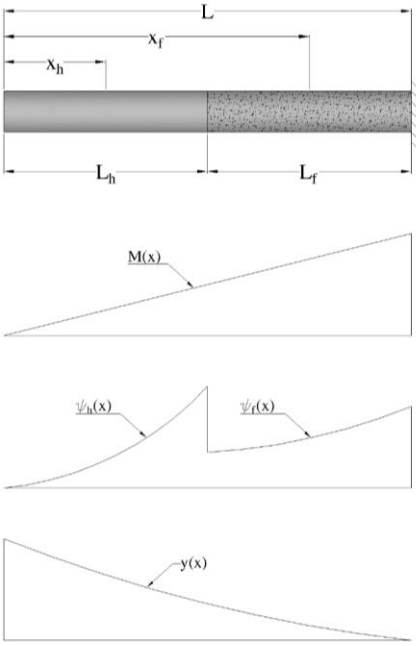

Moment-area theorem

$$y(x) = \int \left(\int \psi(x) dx \right) dx$$

Figure 8: Constructing the load-deflection response from the moment-curvature responses of concrete-filled and hollow sections

2.4 Model Validation

The analytical model was used to predict the load-deflection, load-strain, and moment-curvature responses of all experimental specimens. Fig. 9 shows a comparison between the experimental and analytical load-deflection responses, while Fig. 10 compares the load-axial strain responses at the fixed base and at the end of hollow part between the experimental and analytical results for the third group with diameter 202 mm. The model generally predicts the behaviour well. The analytical model was used to predict the optimal ratio of partial concrete filling after which there is no gain on the maximum failure load. The model was applied on the three tested groups but with a wider range of concrete filling ratios. Fig. 11 compares the ultimate load versus concrete-filling length ratio from the experimental program which are shown as points and the model predictions. Complete curves for the relationship between ultimate load and the percent

of concrete filling ratio were established using the model, in order to establish an accurate prediction of the optimal filling length ratio.

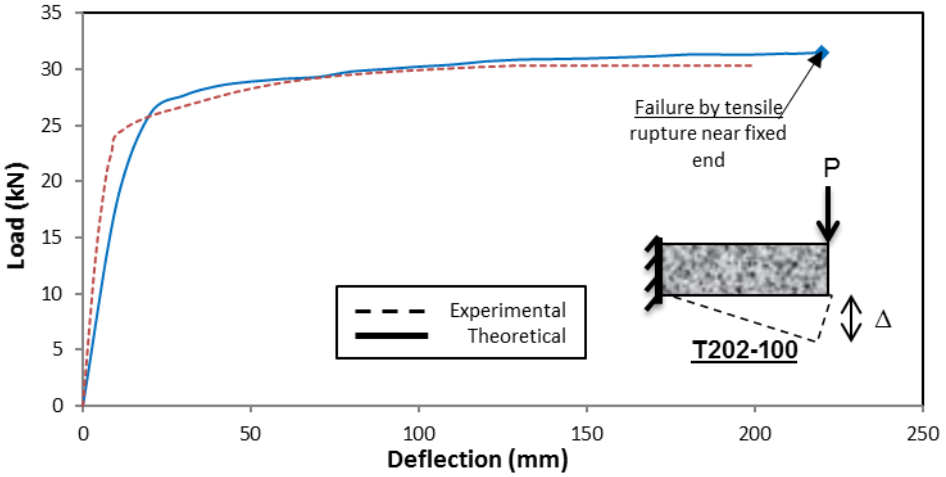

(a)

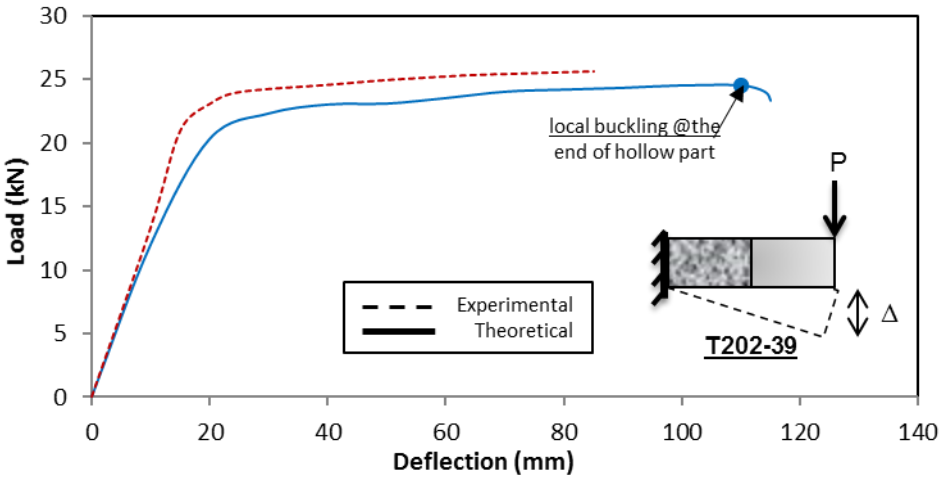

(b)

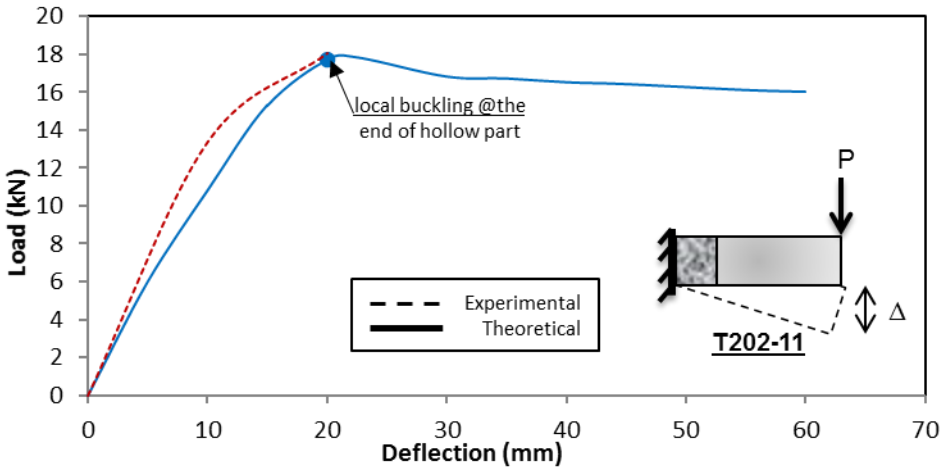

(c)

Figure 9: Experimental and theoretical Load-deflection behavior of the 3rd group with 202 mm diameter

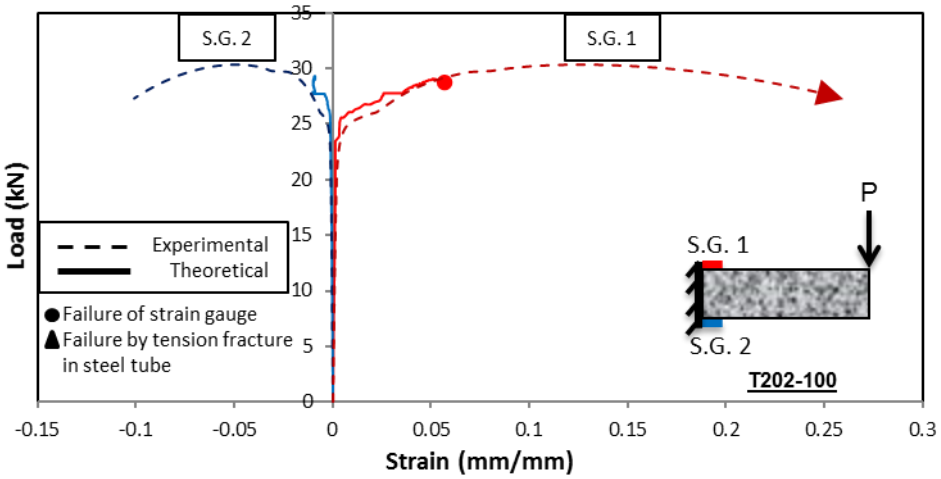

(a)

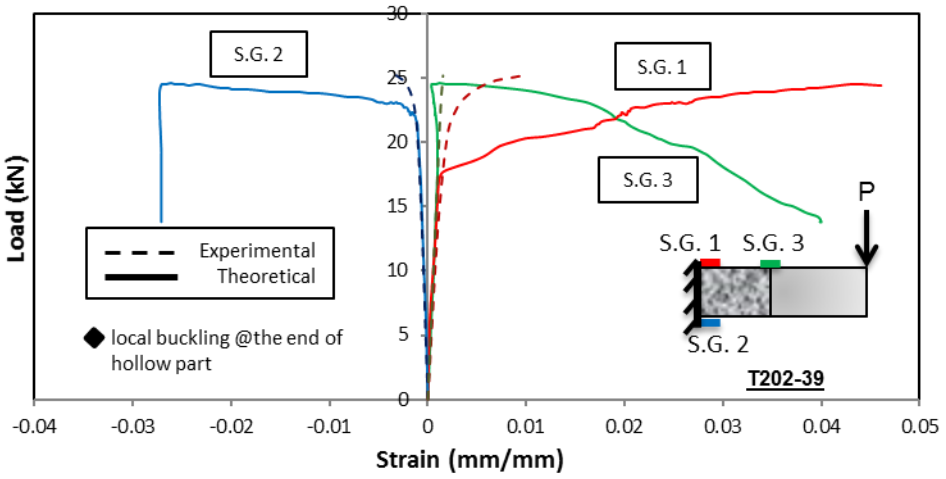

(b)

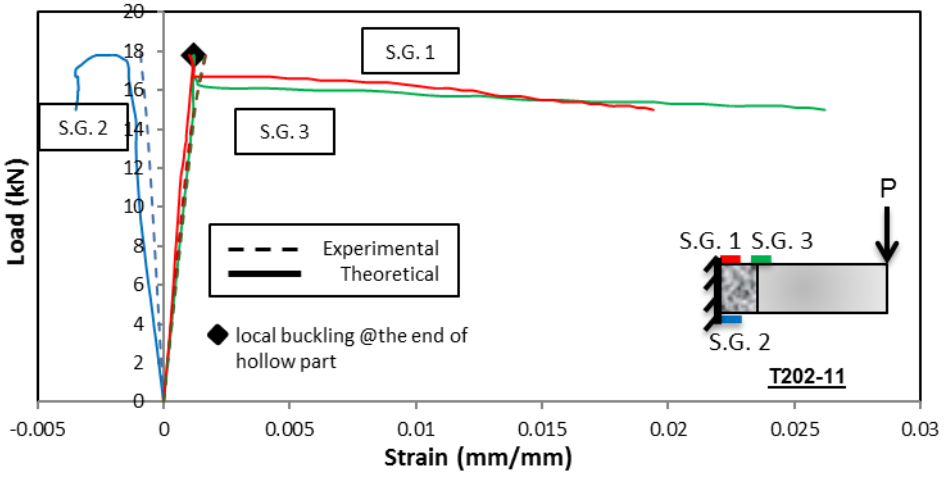

(c)

Figure 10: Experimental and theoretical Load-strain behavior of the 3rd group with 202 mm diameter

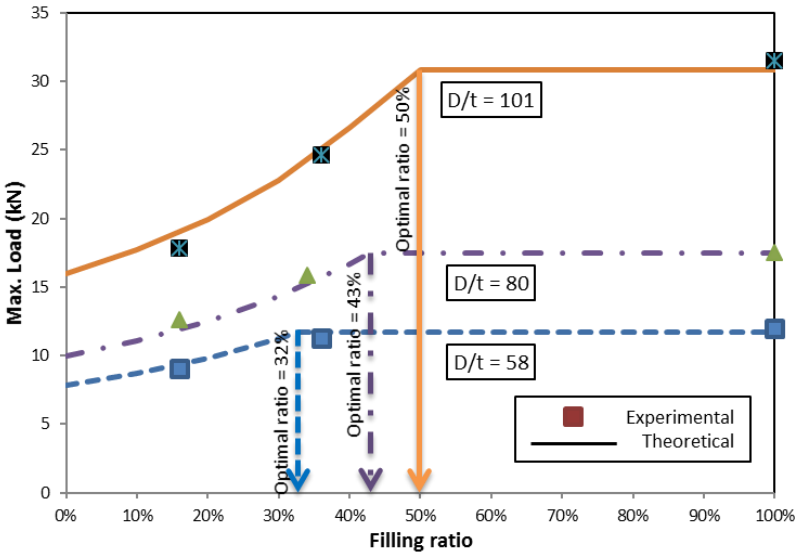

Figure 11: Variation of ultimate load with concrete fill length ratio

3. Parametric Study

The analytical model has been used in a parametric study to investigate the effects of steel grades and diameter-to-wall thickness ratios (D/t) on the optimal filling length ratio of poles loaded by a point load at the free end. The study included three grades of steel (S235, S355 and S420) with different yield-to-ultimate strength ratios (F_y/F_u) as follows: 235/360, 355/470, and 420/500 (MPa/MPa). For each steel grade, different (D/t) ratios are studied to cover the range of non-compact classification according to ANSI/AISC 360-16, which ranges from 0.07 E/F_y to 0.31 E/F_y. So, the studied ranges of D/t ratios were 63 to 277, 41 to 183 and 35 to 155 for the three studied grades of steel, respectively, with an increment of 10. Normal strength concrete is assumed as F_c'=25 MPA.

The study investigated seven wall thicknesses 1, 1.5, 2, 2.5, 3, 3.5, and 4 mm. It's noted that the specimens which have the same D/t ratio and different thickness produce the same optimal length. Figure 12 shows the variation of optimal concrete filling ratio with D/t ratio for the three steel grades used in the study. The optimal ratio from this curve should be increased with 0.5D/L, as it's noted in the experimental tests that the failure of some specimens happened after the end of concrete with a distance 0.5D inside the filled portion.

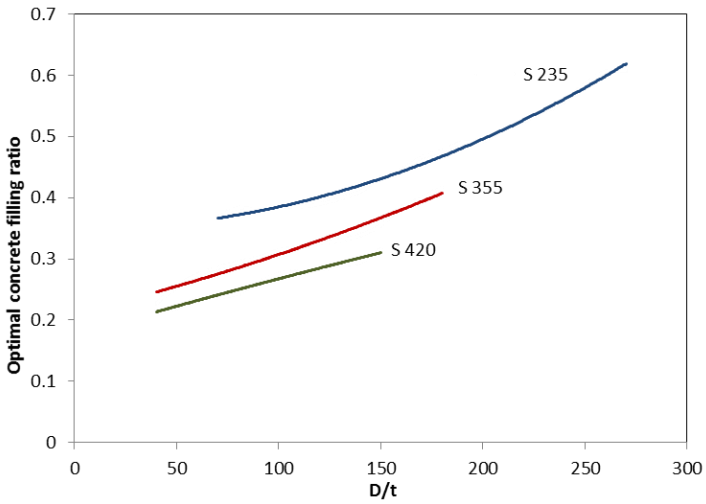

Figure 12: Variation of optimal concrete filling ratio with D/t ratio for various steel grades

Summary and Conclusions

In this paper, an experimental and analytical investigation has been carried out on cantilevered steel tubular poles with partial concrete filling, under bending loading. The lengths of the concrete fill measured from the fixed end are varied among the specimens. Test results showed that as the length of concrete fill increases, the ultimate load gradually increases until it reaches a plateau. As such, there is an optimum length of the partial concrete filling, which depends on D/t and F_y/F_u ratios. This length would result in achieving maximum flexural strength at a minimum dead weight. Tubes having less concrete than optimal failed prematurely within the hollow part by local buckling at the end of the concrete filling. On the other hand, tubes having more concrete than optimal failed within the concrete-filled part at the fixed base by tensile fracture of the tube. An analytical model was developed to predict the behavior of partially concrete-filled poles. The model was validated using the test results and generally showed reasonable agreement. The study showed that the optimum length of the partial concrete fill increases as the (D/t) ratio increases.

References

ANSI/AISC 360-16, "Specification for Structural Steel Buildings", American Institute of Steel Construction, INC., Chicago, Illinois 60601-1802.

Brazier, L.G. (1927). "On the flexure of thin cylindrical shells and other thin sections" proceedings of the Royal Society, Series A, Vol. CXVI, pp. 104-114.

Popovics, S. (1973) "A numerical approach to the complete stress-strain curve of concrete," Cement and Concrete Research, 3 (5), pp.583-599.

Elchalakani, M., Zhao, X.L., Grzebieta, R.H. (2001) "Concrete-filled circular steel tubes subjected to pure bending" Journal of Constructional Steel Research, 57, pp. 1141-1168.

Fam, A.Z., Rizkalla, S.H. (2002) "Flexural behavior of concrete-filled fiber-reinforced polymer circular tubes." Journal of Composites for Construction, 6 (2), pp. 123-132

Guarracino, F. (2003) "On the analysis of cylindrical tubes under flexure: theoretical formulations, experimental data, and finite element analyses" Journal of Thin-Walled Structures 41, pp. 127-147.

Ibrahim, S., Polyzois, D., (1999) "Ovalization analysis of fibre-reinforced plastic poles" Composite Structures, 45 (1), pp. 7-12.

Korol, M. (1979) "Critical buckling strains of round tubes in flexure" International Journal of Mechanical Sciences 21, pp. 719-730.

Mitchell, J.R., Fam, A.Z. (2010) "Tests and Analysis of Cantilevered GFRP Tubular Poles with Partial Concrete Filling" Journal of Composites for Construction, 14 (1), pp. 115-124.